

# Electron-positron annihilation into three pions and the radiative return. <sup>\*</sup>

Henryk Czyż<sup>1 a</sup>, Agnieszka Grzelińska<sup>2 b</sup>, Johann H. Kühn<sup>2 c</sup>, and Germán Rodrigo<sup>3 d</sup>

<sup>1</sup> Institute of Physics, University of Silesia, PL-40007 Katowice, Poland.

<sup>2</sup> Institut für Theoretische Teilchenphysik, Universität Karlsruhe, D-76128 Karlsruhe, Germany.

<sup>3</sup> Instituto de Física Corpuscular, CSIC-Universitat de València, Apartado de Correos 22085, E-46071 Valencia, Spain.

May 2, 2006

**Abstract.** The Monte Carlo event generator PHOKHARA, which simulates hadron and muon production at electron-positron colliders through radiative return, has been extended to final states with three pions. A model for the form factor based on generalized vector dominance has been employed, which is consistent with presently available experimental observations.

## 1 Introduction

Measurements of form factors and cross sections for electron positron annihilation in the low energy region provide important information on hadron dynamics. At the same time, they are necessary ingredients in dispersion relations, which are used to predict hadronic contributions to the momentum dependent electromagnetic coupling and the anomalous magnetic moment of the muon. The measurements are traditionally performed by tuning the center of mass energy of an electron positron collider to the point of interest. As an alternative, it has been advocated to use the method of the radiative return [1,2] at high luminosity  $\phi$ - and  $B$ -meson factories. In this second case the collider energy remains fixed, while  $Q^2$ , the invariant mass of the hadronic system, can be varied by considering events, where one or several photons have been radiated. For a detailed and precise analysis initial and final state radiation must be included and a proper description of the various exclusive final states through appropriate form factors is required. All these ingredients are contained in

the most recent version of the Monte Carlo event generator PHOKHARA4.0 [3,4], which is based in particular on the virtual corrections described in [5,6] and which at present simulates production of  $\mu^+\mu^-$ ,  $\pi^+\pi^-$ , four pions ( $2\pi^+2\pi^-$  and  $\pi^+\pi^-2\pi^0$ ),  $p\bar{p}$ , and  $n\bar{n}$  [3,4,5,6,7,8,9]. In the present work the production of three pions is considered on the basis of form factors, which include already available information on the production cross section and on differential distributions in two-pion subsystems. The model implements three-pion production through  $\omega$ ,  $\phi$  and their radial excitations and the subsequent decay of these resonances into  $\rho\pi$ ,  $\rho'\pi$  and  $\rho''\pi$ . A small isospin-violating component  $\gamma^* \rightarrow \omega(\rightarrow \pi^+\pi^-)\pi^0$  is added, which is needed to properly describe the data. The total cross section and the distributions are well reproduced within this model. It is furthermore demonstrated that the couplings introduced and adopted for this purpose lead to a satisfactory description of  $\Gamma(\pi^0 \rightarrow \gamma\gamma)$ , of the slope parameter of the  $\pi^0 \rightarrow \gamma\gamma^*$  amplitude and of the radiative vector meson decays  $\rho \rightarrow \pi^0\gamma$ ,  $\phi \rightarrow \pi^0\gamma$ , but is in conflict with  $\omega \rightarrow \pi^0\gamma$ .

## 2 A phenomenological description of three-pion production

The amplitude for three-pion production through the electromagnetic current is restricted by current conservation and negative parity to the form

$$\begin{aligned} J_\nu^{\text{em},3\pi} &= \langle \pi^+(q_+) \pi^-(q_-) \pi^0(q_0) | J_\nu^{\text{em}} | 0 \rangle \\ &= \epsilon_{\nu\alpha\beta\gamma} q_+^\alpha q_-^\beta q_0^\gamma F_{3\pi}(q_+, q_-, q_0) . \end{aligned} \quad (1)$$

<sup>\*</sup> Work supported in part by BMBF under grant number 05HT4VKA/3, EC 5th Framework Programme under contract HPRN-CT-2002-00311 (EURIDICE network), TARI project RII3-CT-2004-506078, Polish State Committee for Scientific Research (KBN) under contract 1 P03B 003 28, Ministerio de Educación y Ciencia under grant FPA2004-00996 (PARSIFAL), and Generalitat Valenciana (GV05-015, GV04B-594 and GRUPOS03/013).

<sup>a</sup> e-mail: czyz@us.edu.pl

<sup>b</sup> e-mail: grzel@joy.phys.us.edu.pl

<sup>c</sup> e-mail: johann.kuehn@uni-karlsruhe.de

<sup>d</sup> e-mail: german.rodrido@ific.uv.es

G-parity dictates dominance of the isospin-zero component of the electromagnetic current, which will be discussed in a first step. The small isospin-one admixture will be discussed subsequently. The form factor  $F_{3\pi}^{I=0}$  is constructed under the assumption that the virtual photon couples to the  $\omega$ - and  $\phi$ -meson, whose subsequent transition to three pions is dominated by the  $\rho(\rightarrow 2\pi)\pi$  chain (Fig.1) [10]. Taking into account radial excitations of  $\omega$ ,  $\phi$ ,  $\rho$  one arrives at the form factor

$$F_{3\pi}^{I=0}(q_+, q_-, q_0) = \sum_{i,j} a_{ij} \cdot BW_{V_i}(Q^2) \cdot H_{\rho_j}(Q_+^2, Q_-^2, Q_0^2), \quad (2)$$

where  $V_i$  stands for either  $\omega$ - or  $\phi$ -resonances, and  $\rho_j$  represents contributions from  $\rho$ -mesons. From the PDG [11] it

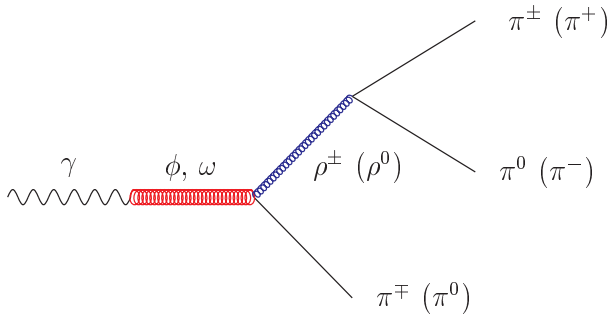


**Fig. 1.** Diagrams contributing to the 3-pion current:  $I = 0$  component.

is clear that all  $\omega$ - and  $\phi$ -resonances couple to the ground state of the  $\rho$ -meson, whereas there is no indication about couplings to the higher radial excitations ( $\rho', \rho'', \dots$ ). This missing piece of information can, however, be obtained to large extent from the known  $e^+e^- \rightarrow \pi^+\pi^-\pi^0$  cross section, as shown below.

For the function  $H_\rho$  we shall adopt the ansatz

$$H_\rho(Q_+^2, Q_-^2, Q_0^2) = BW_\rho(Q_0^2) + BW_\rho(Q_+^2) + BW_\rho(Q_-^2), \quad (3)$$

with

$$Q_0^2 = (q_+ + q_-)^2, \quad Q_\pm^2 = (q_\mp + q_0)^2, \quad (4)$$

and the Breit-Wigner form factors are

$$BW_V(Q^2) = \left[ \frac{Q^2}{m_V^2} - 1 + i \frac{\Gamma_V}{m_V} \right]^{-1},$$

$$BW_\rho(Q_i^2) = \left[ \frac{Q_i^2}{m_\rho^2} - 1 + i \frac{\sqrt{Q_i^2} \Gamma_\rho(Q_i^2, m_j, m_k)}{m_\rho^2} \right]^{-1}, \quad (5)$$

where  $Q_i^2 = (q_j + q_k)^2$ , and  $m_j = m_{\pi^j}$ , with  $i, j, k = 0, \pm$ . We use propagators with constant widths for  $\omega$ 's and  $\phi$ , and energy dependent widths for  $\rho$ -resonances as predicted by P-wave  $\rho \rightarrow \pi\pi$  decays:

$$\Gamma_\rho(Q_i^2, m_j, m_k) = \Gamma_\rho \frac{m_\rho^2}{Q_i^2} \left[ \frac{Q_i^2 - (m_j + m_k)^2}{m_\rho^2 - (m_j + m_k)^2} \right]^{3/2}. \quad (6)$$

The couplings  $a_{ij}$  are taken as real constants and we assume that the isospin symmetry is violated in this component only by the  $\pi^0 - \pi^\pm$  mass difference.

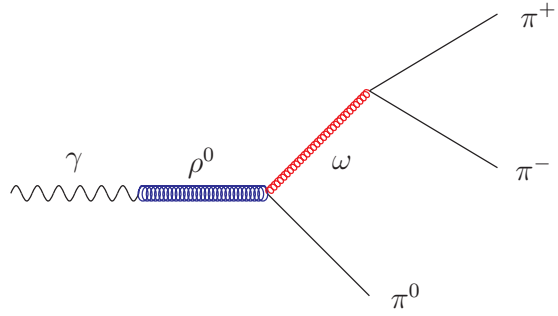


**Fig. 2.** Diagram contributing to the  $I = 1$  component of the three-pion current.

The small isospin violating amplitude is mediated by the  $I = 1$  component of the electromagnetic current and is based on the  $4\pi$  current of Refs. [12, 13] i.e. we take the  $\rho - \gamma$  and  $\rho\pi\omega$  couplings from the  $4\pi$  current and replace the  $\omega \rightarrow 3\pi$  transition by the isospin violating  $\omega \rightarrow 2\pi$  decay as shown in Fig.2. This leads to the following ansatz

$$F_{3\pi}^{I=1}(q_+, q_-, q_0) = G_\omega \cdot BW_\omega(Q^2) / \tilde{m}_\omega^2 [BW_\rho(Q_0^2) / \tilde{m}_\rho^2 + \sigma BW_{\rho'}(Q_0^2) / \tilde{m}_{\rho'}^2], \quad (7)$$

where

$$G_\omega = \frac{1.55}{\sqrt{2}} 12.924 \text{ GeV}^{-1} 0.266 m_\rho^2 g_{\omega\pi\pi} \quad (8)$$

and  $\tilde{m}_\rho = 0.77609 \text{ GeV}$ ,  $\tilde{\Gamma}_\rho = 0.14446 \text{ GeV}$ ,  $\tilde{m}_{\rho'} = 1.7 \text{ GeV}$ ,  $\tilde{\Gamma}_{\rho'} = 0.26 \text{ GeV}$ ,  $\sigma = -0.1$ , where the parameters are taken directly from [13]. At the present level of experimental accuracy it is not clear whether the  $\rho'$  term is necessary for the description of the  $3\pi$  current (see below). However, as it is a prediction coming from the  $4\pi$  current we consider its contribution also here.

The coupling  $g_{\omega\pi\pi}$  can be extracted from the decay rate  $\Gamma(\omega \rightarrow \pi\pi)$  (see Eq.(12)). Using the world average value from the PDG [11] one gets  $g_{\omega\pi\pi} = 0.185(15)$ . The total form factor is of course given by the coherent sum

$$F_{3\pi}(q_+, q_-, q_0) = F_{3\pi}^{I=0}(q_+, q_-, q_0) + F_{3\pi}^{I=1}(q_+, q_-, q_0). \quad (9)$$

Data on  $\sigma(e^+e^- \rightarrow \pi^+\pi^-\pi^0)$ , from energy scan experiments [14, 15, 16, 17, 18] consist of 217 data points, covering

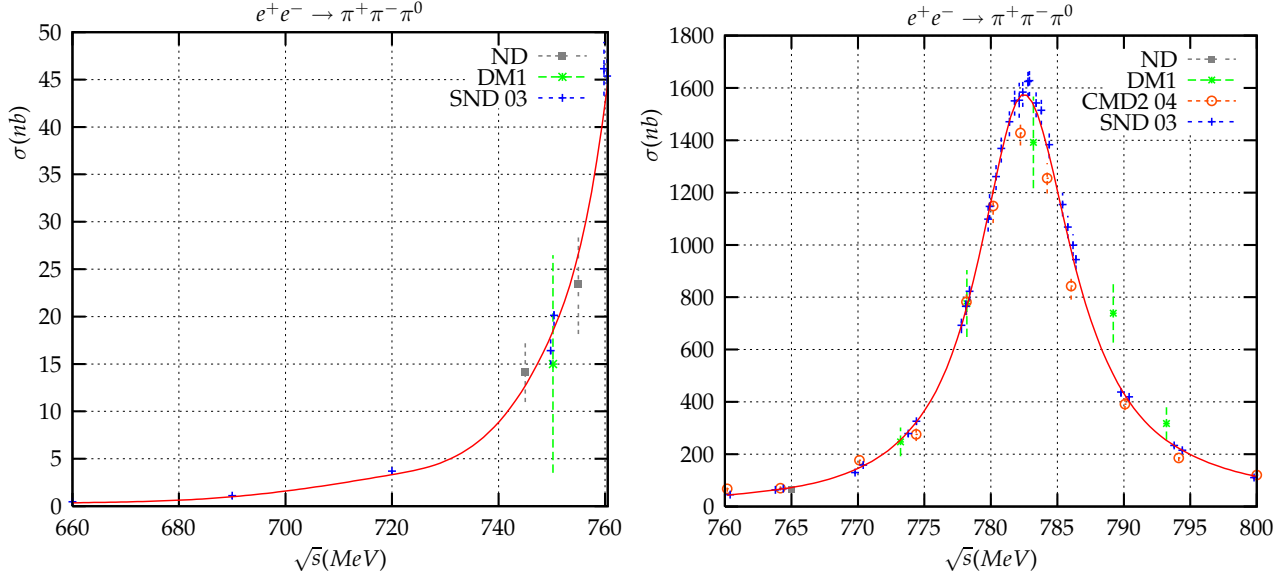


**Fig. 3.**  $e^+e^- \rightarrow \pi^+\pi^-\pi^0$  cross section obtained with fitted parameters (solid line, see text for details) vs. experimental data.

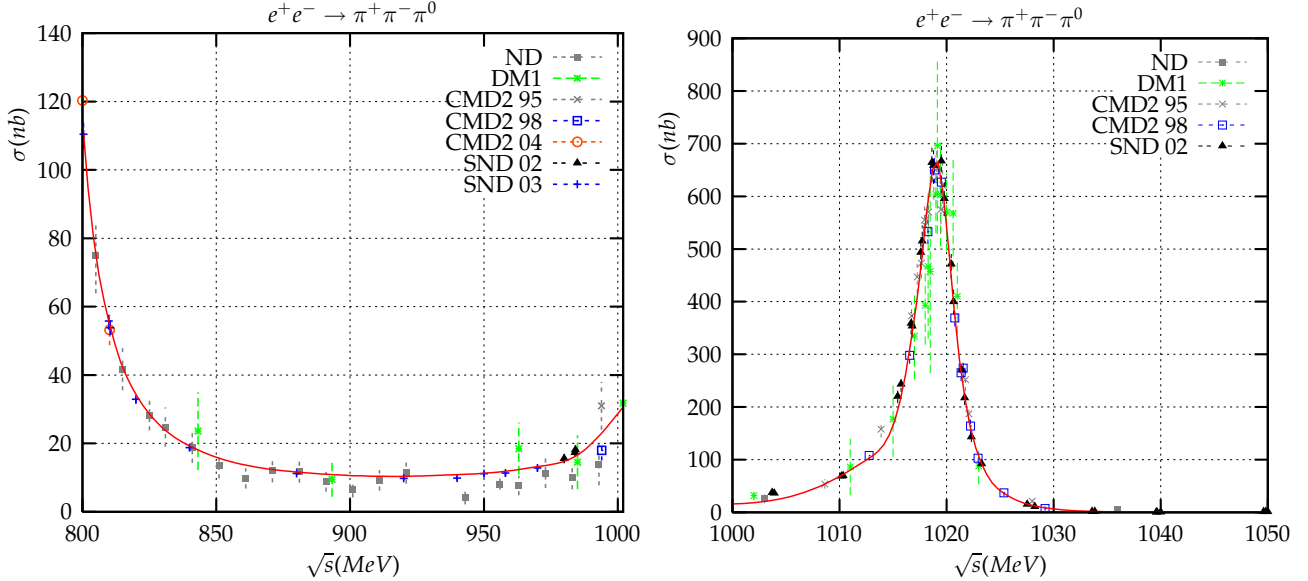


**Fig. 4.**  $e^+e^- \rightarrow \pi^+\pi^-\pi^0$  cross section obtained with fitted parameters (solid line, see text for details) vs. experimental data.

the energy range from 660 MeV to 2400 MeV. Moreover, by using the radiative return method, BaBar [19] has obtained additional 78 data points, covering the energy from 1.06 GeV up to almost 3 GeV. Data from the DM2 collaboration [18] being inconsistent with the more accurate BaBar data, were not used in the fit.

To fit the experimental data we include the following resonances:  $\omega(782)$ ,  $\omega' \equiv \omega(1420)$ ,  $\omega'' \equiv \omega(1650)$ ,  $\phi(1020)$ ,  $\rho(770)$ ,  $\rho' \equiv \rho(1450)$  and  $\rho'' \equiv \rho(1700)$ . The strategy was to minimize the number of contributions in Eq.(2) and arrive at a good fit in the same time. Our best fit for the

isospin zero component reads

$$\begin{aligned}
 F_{3\pi}^{I=0}(q_+, q_-, q_0) = & H_{\rho(770)}(Q_+^2, Q_-^2, Q_0^2) \\
 & \cdot \left[ A \cdot BW_{\omega(782)}(Q^2) + B \cdot BW_{\phi(1020)}(Q^2) \right. \\
 & \left. + C \cdot BW_{\omega(1420)}(Q^2) + D \cdot BW_{\omega(1650)}(Q^2) \right] \\
 & + E \cdot BW_{\phi(1020)}(Q^2) \cdot H_{\rho(1450)}(Q_+^2, Q_-^2, Q_0^2) \\
 & + F \cdot BW_{\omega(1650)}(Q^2) \cdot H_{\rho(1700)}(Q_+^2, Q_-^2, Q_0^2), \quad (10)
 \end{aligned}$$

with the couplings and masses given in Table 1. The errors are the parabolic errors calculated by the MINUIT processor MINOS and correspond to the change of  $\Delta\chi^2 = 1$ .

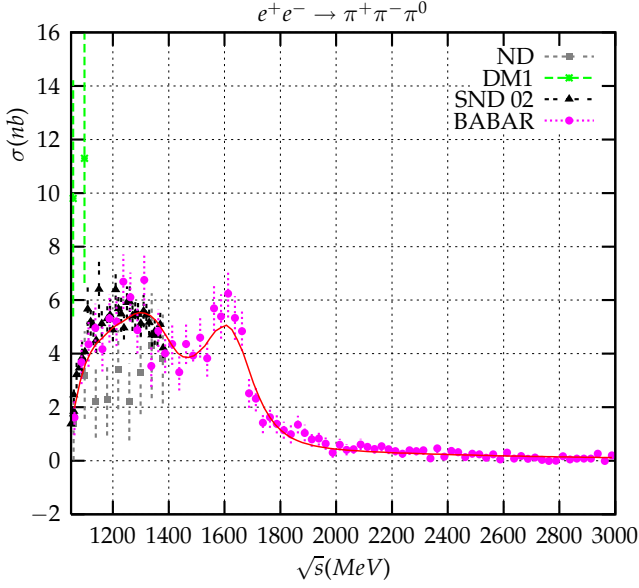


**Fig. 5.**  $e^+e^- \rightarrow \pi^+\pi^-\pi^0$  cross section obtained with fitted parameters (solid line, see text for details) vs. experimental data.

The value  $\chi^2/\text{d.o.f} = 1.14$  is at the edge of the 95% confidence interval. It is to large extent a result of the fact that the data of different experiments are only marginally mutually consistent as evident from Figures 3–5. Lack of published numerical information on differential distributions does not allow for further refinements of the model. In particular, indications for additional contributions from higher radial excitations in the region of large  $Q^2$  cannot be substantiated by more detailed fits. Access to distributions in invariant masses of pion pairs and to pion angular distributions would allow to study these effects. For the moment we set the masses and widths of the  $\rho$  mesons to the values collected in Table 2 and assume equal masses and widths for the neutral and charged  $\rho$  mesons. Nevertheless qualitative comparisons of two-pion invariant mass distributions can be performed by superimposing the experimental and the model (data from Fig. 15 of [19] and differential cross sections generated with PHOKHARA 5.0) distributions (see Fig.6). The  $I = 0$  component alone predicts identical distributions in  $M_{\pi^+\pi^-}$  and  $M_{\pi^\pm\pi^0}$ . The

**Table 1.** Values of the couplings masses and widths obtained in the fit; couplings  $A - F$  in  $\text{GeV}^{-3}$  masses and widths in MeV (see text for details).

$m_\omega(782)$	782.4(4)	$A$	18.20(8)
$\Gamma_\omega(782)$	8.69(7)	$B$	-0.87(5)
$m_\phi(1020)$	1019.24(3)	$C$	-0.77(5)
$\Gamma_\phi(1020)$	4.14(5)	$D$	-1.12(4)
$m_\omega(1420)$	1375(1)	$E$	-0.72(10)
$\Gamma_\omega(1420)$	250(5)	$F$	-0.59(4)
$m_\omega(1650)$	1631(6)		
$\Gamma_\omega(1650)$	245(13)	$\chi^2/\text{d.o.f}$	1.14

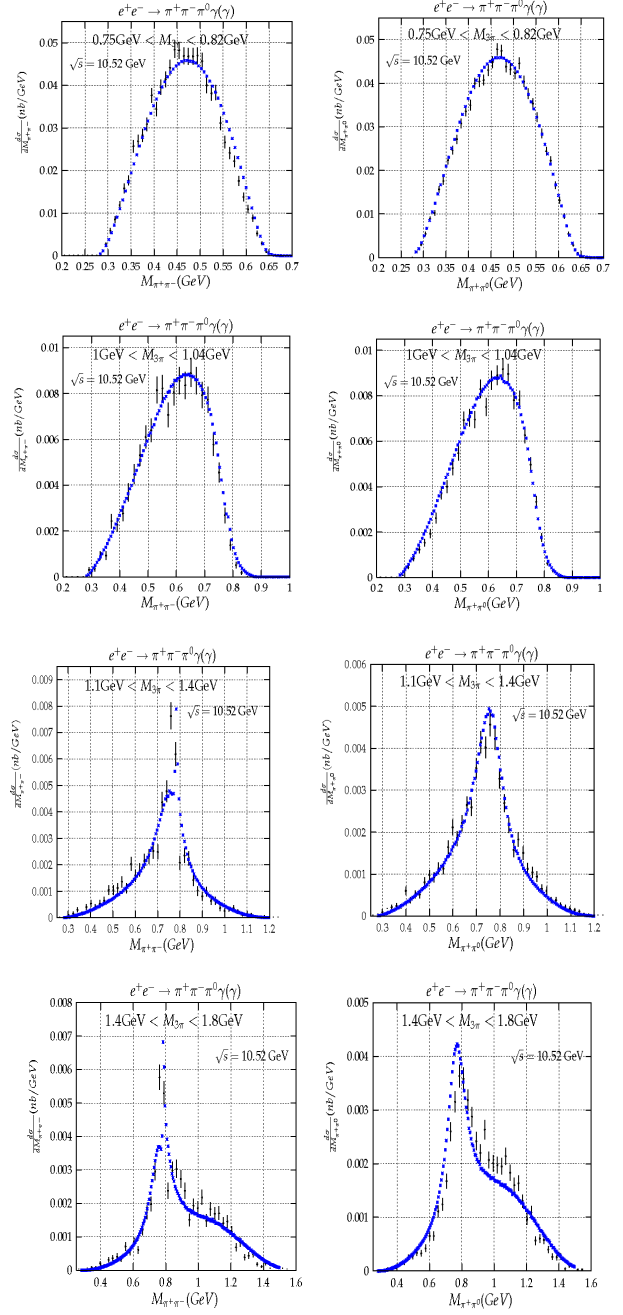


**Fig. 6.** Two pion invariant mass distributions for four different ranges of  $\pi^+\pi^-\pi^0$  invariant mass. The BaBar data points, given as events/bin, are superimposed on plots obtained by PHOKHARA (see text for details).

small  $I = 1$  component is concentrated in the spike at  $M_{\pi^+\pi^-} = m_\omega$ . This channel starts to contribute for  $Q^2$  values above 1 GeV only. The model seems to describe the distributions reasonably well. However the following deviations are observed: In the lowest region ( $0.75 \text{ GeV} < M_{3\pi} < 0.82 \text{ GeV}$ ) the experimental results for the distributions in  $M_{\pi^+\pi^-}$  and  $M_{\pi^\pm\pi^0}$ , respectively, seem to differ in the upper range, an indication of isospin-violation,

**Table 2.** The masses and widths of  $\rho$  resonances used in the fits

	$\rho(770)$	$\rho(1450)$	$\rho(1700)$
$m$ (GeV)	0.77609	1.465	1.7
$\Gamma$ (GeV)	0.14446	0.31	0.235

that cannot be reproduced by our ansatz. In the large  $Q^2$  range ( $1.4 \text{ GeV} < M_{3\pi} < 1.8 \text{ GeV}$ ) an excess is observed in both charge modes for masses of the two-pion system between 1 GeV and 1.2 GeV. A similar excess is not observed in the pion form factor.

### 3 Meson couplings and partial decay widths.

From the results of the fit we can evaluate the meson couplings separately, combining the following relations

$$\begin{aligned}
A &= 2g_{\omega\gamma} \cdot g_{\omega\pi\rho} \cdot g_{\rho\pi\pi} \\
B &= 2g_{\phi\gamma} \cdot g_{\phi\pi\rho} \cdot g_{\rho\pi\pi} \\
C &= 2g_{\omega'\gamma} \cdot g_{\omega'\pi\rho} \cdot g_{\rho\pi\pi} \\
D &= 2g_{\omega''\gamma} \cdot g_{\omega''\pi\rho} \cdot g_{\rho\pi\pi} \\
E &= 2g_{\phi\gamma} \cdot g_{\phi\pi\rho'} \cdot g_{\rho'\pi\pi} \\
F &= 2g_{\omega''\gamma} \cdot g_{\omega''\pi\rho''} \cdot g_{\rho''\pi\pi}, \quad (11)
\end{aligned}$$

with information about partial decay widths. From the known decay widths of  $\rho^0, \omega$  and  $\phi$  to two pions one determines the couplings  $g_{V\pi\pi}$  ( $V = \rho^0, \omega, \phi$ ):

$$\Gamma_{V \rightarrow \pi^+\pi^-} = g_{V\pi\pi}^2 \frac{m_V}{48\pi} \left[ 1 - \frac{4m_{\pi^+}^2}{m_V^2} \right]^{3/2}. \quad (12)$$

Similarly, the  $g_{V\gamma}$  couplings can be found from the measured values of  $\Gamma(V \rightarrow e^+e^-)$ :

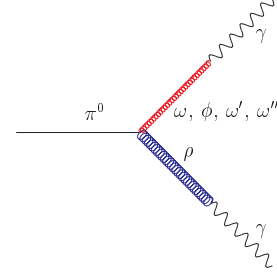
$$\Gamma_{V \rightarrow e^+e^-} = g_{V\gamma}^2 \frac{4\pi\alpha^2}{3m_V^3}. \quad (13)$$

For the  $\omega'$  and  $\omega''$  we do not know the partial decay widths and the couplings cannot be extracted separately. The numerical values of the couplings obtained from Eq.(11) and partial decay widths [11] are collected in Table 3.

**Table 3.** Values of the three- and two-particle couplings;  $g_{V\pi\pi}$  is dimensionless,  $g_{V\gamma}$  in  $\text{GeV}^2$ ,  $g_{V\rho}$  in  $\text{GeV}^{-5}$ .

$g_{\rho\pi\pi}$	5.997(32)	$g_{\rho\gamma}$	0.1212(13)
$g_{\omega\pi\pi}$	0.185(15)	$g_{\omega\gamma}$	0.03591(37)
$g_{\phi\pi\pi}$	0.0072(6)	$g_{\phi\gamma}$	0.0777(7)
$g_{\omega\pi\rho}$	42.3(5)	$g_{\omega'\gamma} \cdot g_{\omega'\pi\rho}$	-0.064(8)
$g_{\phi\pi\rho}$	-0.93(5)	$g_{\omega''\gamma} \cdot g_{\omega''\pi\rho}$	-0.093(3)

Having extracted the couplings, we are able to predict many physical quantities that have been measured already and check the model. In particular we will investigate if

**Fig. 7.** Diagrams contributing to  $\pi^0 \rightarrow \gamma\gamma$  decay.

various meson–photon interactions can be modeled, as in the  $3\pi$  case, by three–meson couplings and vector meson–photon mixings with the couplings and propagators as introduced above (for a review of alternative models see [20, 21]). As one can recognize our model is an extension to higher radial excitations of the model outlined in [10].

Let us start with the decay width of  $\pi^0 \rightarrow \gamma\gamma$ . The model is based on the diagrams shown in Fig.7. As indicated by the fit, contributions from  $\rho' - \gamma$  and  $\rho'' - \gamma$  mixings are not required at the present level of precision.

**Table 4.** Mean life time for  $\pi^0 \rightarrow 2\gamma$  in seconds and decay rates for  $\rho, \omega, \phi \rightarrow \pi^0\gamma$  in MeV as obtained within our model compared to experimental results [11].

	model	experiment
$\tau(\pi^0 \rightarrow \gamma\gamma)$	$6.6(3) \cdot 10^{-17}$	$8.3(6) \cdot 10^{-17}$
$\Gamma(\rho^0 \rightarrow \pi^0\gamma)$	0.078(3)	0.090(20)
$\Gamma(\omega \rightarrow \pi^0\gamma)$	1.31(4)	$0.757^{+25}_{-22}$
$\Gamma(\phi \rightarrow \pi^0\gamma)$	$4.2(5) \cdot 10^{-3}$	$5.2(4) \cdot 10^{-3}$

The partial decay width of the decay  $\pi^0 \rightarrow \gamma\gamma$  is thus given in our model by

$$\Gamma_{\pi^0 \rightarrow \gamma\gamma} = \pi\alpha^2 m_{\pi^0}^3 g_{\rho\gamma}^2 T^2, \quad (14)$$

with

$$T = g_{\omega\pi\rho} \cdot g_{\omega\gamma} + g_{\phi\pi\rho} \cdot g_{\phi\gamma} + g_{\omega'\pi\rho} \cdot g_{\omega'\gamma} + g_{\omega''\pi\rho} \cdot g_{\omega''\gamma} \quad (15)$$

This ansatz leads to  $\tau_{\pi^0} = 6.6(3) \cdot 10^{-17} \text{ s}$  for the  $\pi^0 \rightarrow \gamma\gamma$  lifetime to be compared with the PDG [11] value  $\tau_{\pi^0} = 8.3(6) \cdot 10^{-17} \text{ s}$ . The  $\omega'$  and  $\omega''$  contributions are small but not negligible and the value of the  $\pi^0$  lifetime obtained without them reads  $\tau_{\pi^0}(\omega \text{ and } \phi \text{ only}) = 5.21(13) \cdot 10^{-17} \text{ s}$ . Within two and a half standard deviations experiment and the model are in agreement ( $experiment - model = (1.7 \pm 0.7) \cdot 10^{-17} \text{ s}$ ) and the remaining discrepancy can be attributed to the missing  $\rho$ -resonances or a more complicated  $Q^2$ -dependence of the propagators. One has to remember that we make here extrapolation from the region of  $\omega, \phi, \dots$  resonances where the fit was performed to the region of the applicability of the chiral limit. Thus

we should recover here the chiral theory result for the  $\pi^0 \rightarrow \gamma\gamma$  lifetime (see [20])

$$\Gamma(\pi^0 \rightarrow \gamma\gamma) = \frac{\alpha^2 m_{\pi^0}^3}{32\pi^3 f^2}, \quad (16)$$

which gives  $\tau_{\pi^0} = 8.69 \cdot 10^{-17}$  s for  $f=132$  MeV. Rephrasing the same statement using the coupling constants one approximately expects

$$\frac{1}{32\pi^4 f^2} \simeq g_{\rho\gamma}^2 T^2 + \dots, \quad (17)$$

where the dots correspond to terms neglected in modelling of the  $3\pi$  current. The discrepancy indicates that extending the validity of our model beyond the description of the  $3\pi$  current one should probably take into account further contributions. However the  $2.5 \sigma$  discrepancy does not allow to draw any final conclusion.

The amplitude of the process  $\pi^0 \rightarrow \gamma\gamma^*$  for small values of the four momentum of the off shell photon can be parameterized by a slope parameter  $\alpha$

$$\mathcal{M}_{\pi^0 \rightarrow \gamma\gamma^*} = \mathcal{M}_{\pi^0 \rightarrow \gamma\gamma} (1 + \alpha k^{*2}). \quad (18)$$

Expanding the Breit-Wigner propagators one obtains

$$\alpha = \frac{1}{2} \left( \frac{1}{m_\rho^2} + \frac{g_{\omega\pi\rho} \cdot g_{\omega\gamma}}{T m_\omega^2} + \frac{g_{\phi\pi\rho} \cdot g_{\phi\gamma}}{T m_\phi^2} + \frac{g_{\omega'\pi\rho} \cdot g_{\omega'\gamma}}{T m_{\omega'}^2} + \frac{g_{\omega''\pi\rho} \cdot g_{\omega''\gamma}}{T m_{\omega''}^2} \right), \quad (19)$$

where  $T$  is defined in Eq.(15). Numerically this gives  $\alpha = 1.74(2)$  GeV<sup>-2</sup>, or  $\alpha \cdot m_{\pi^0}^2 = 0.0317(5)$ , to be compared with the experimental value [11]  $\alpha \cdot m_{\pi^0}^2 = 0.032(4)$ .

The model also predicts the decay rates for the  $\rho^0 \rightarrow \pi^0\gamma$ ,  $\omega \rightarrow \pi^0\gamma$  and  $\phi \rightarrow \pi^0\gamma$ :

$$\Gamma_{\rho^0 \rightarrow \pi^0\gamma} = \frac{\alpha}{24} m_\rho^5 \left[ 1 - \frac{m_{\pi^0}^2}{m_\rho^2} \right]^3 \cdot T^2 \quad (20)$$

$$\Gamma_{V \rightarrow \pi^0\gamma} = \frac{\alpha}{24} m_V^5 \left[ 1 - \frac{m_{\pi^0}^2}{m_V^2} \right]^3 g_{V\pi\rho}^2 \cdot g_{\rho\gamma}^2, \quad (21)$$

where  $V$  stands for  $\omega$  or  $\phi$ . The results are collected in Table 4 and compared with the respective experimental values.

In the  $\rho^0 \rightarrow \pi^0\gamma$  decay our prediction for this branching ratio  $5.2(2) \cdot 10^{-4}$  is in agreement with the  $6.0(1.3) \cdot 10^{-4}$  of [11] within  $1\sigma$ . As the only isospin violating effect in our model for this process is the charged-neutral pion mass difference, our prediction for the  $\text{Br}(\rho^\pm \rightarrow \pi^\pm\gamma) = 5.2(2) \cdot 10^{-4}$  is identical (within the errors) with the one for the neutral mode and is also in agreement with the data [11]  $\text{Br}(\rho^\pm \rightarrow \pi^\pm\gamma) = 4.5(5) \cdot 10^{-4}$ .

For the  $\phi \rightarrow \pi^0\gamma$  decay the branching ratio  $\text{Br}(\phi \rightarrow \pi^0\gamma) = 0.99(12) \cdot 10^{-3}$  is in agreement within  $2\sigma$  with the value  $1.23(12) \cdot 10^{-3}$  from Ref. [11]. Our result for

$\text{Br}(\omega \rightarrow \pi^0\gamma) = 15.4(5)\%$  overestimates however the measured value  $((8.92_{-0.24}^{+0.28})\%)$  by factor 1.7.

The extracted couplings determine also the cross section of the reaction  $e^+e^- \rightarrow \pi^0\gamma$ ,

$$\begin{aligned} \sigma(e^+e^- \rightarrow \pi^0\gamma) &= \frac{2\pi^2\alpha^3}{3} \left( 1 - \frac{m_{\pi^0}^2}{s} \right)^3 g_{\rho\gamma}^2 \\ &\cdot \left| [g_{\omega\pi\rho} \cdot g_{\omega\gamma} + g_{\phi\pi\rho} \cdot g_{\phi\gamma} \right. \\ &\quad + g_{\omega'\pi\rho} \cdot g_{\omega'\gamma} + g_{\omega''\pi\rho} \cdot g_{\omega''\gamma}] \cdot BW_\rho(s) \\ &\quad + g_{\omega\gamma} \cdot g_{\omega\pi\rho} \cdot BW_\omega(s) + g_{\phi\gamma} \cdot g_{\phi\pi\rho} \cdot BW_\phi(s) \\ &\quad \left. + g_{\omega'\pi\rho} \cdot g_{\omega'\gamma} \cdot BW_{\omega'}(s) + g_{\omega''\pi\rho} \cdot g_{\omega''\gamma} \cdot BW_{\omega''}(s) \right|^2, \end{aligned} \quad (22)$$

with  $BW_i$ ,  $i = \rho, \omega, \phi, \omega', \omega''$  defined in Eq.(5).

The comparison with existing data [23,24] is shown in Fig. 8, where one standard deviation bands are given. Reasonable agreement is observed around the  $\phi$  resonance in contrast to the  $\omega$  region. This is of course a reflection of the agreement and disagreement of the corresponding decay rates. A similar behaviour was also observed in Ref. [22]. Their model predict a value for  $\Gamma(\omega \rightarrow \pi^0\gamma)$  well in accordance with the experimental value, but could not easily reproduce  $\Gamma(\omega \rightarrow \pi^+\pi^-\pi^0)$ . Further, both theoretical and experimental, studies of reactions  $e^+e^- \rightarrow \pi^+\pi^-\pi^0$  and  $e^+e^- \rightarrow \pi^0\gamma$  are thus required.

The branching ratios of the  $\omega$ ,  $\phi$  and  $\rho$  decays to  $\pi^+\pi^-\pi^0$  obtained within our model can be found in Table 5. They are in agreement with the PDG values [11] for  $\omega$ ,  $\phi$  within 1-2 standard deviations. However the predicted value for  $\text{Br}(\rho^0 \rightarrow \pi^+\pi^-\pi^0)$  is more then two orders of magnitude smaller than the experimental value  $\text{Br}(\rho^0 \rightarrow \pi^+\pi^-\pi^0) \simeq 1 \cdot 10^{-4}$ , which is consistent with zero at two sigma level.

**Table 5.** Branching ratios of the  $\omega$ ,  $\phi$  and  $\rho$  to  $\pi^+\pi^-\pi^0$  decays: model vs. experiment [11].

	model	experiment
$\text{Br}(\omega \rightarrow \pi^+\pi^-\pi^0)$	95.1(22)%	89.1(7)%
$\text{Br}(\phi \rightarrow \pi^+\pi^-\pi^0)$	14.5(22)%	15.4(5)%
$\text{Br}(\rho \rightarrow \pi^+\pi^-\pi^0)$	$1.9(3) \cdot 10^{-6}$	$(1.01_{-0.36}^{+0.54} \pm 0.34) \cdot 10^{-4}$

## 4 Tests of the MC code

In comparison to the previous versions of PHOKHARA the default random number generator was changed to the double precision version of RANLUX [25] written in C by Martin Lüscher. A C-FORTRAN interface is provided with the PHOKHARA 5.0 distribution.

To assure a technical precision of the code better than a fraction of one per mille a number of tests were performed for the new hadronic state in the generator. Among other tests, the initial state emission was tested against

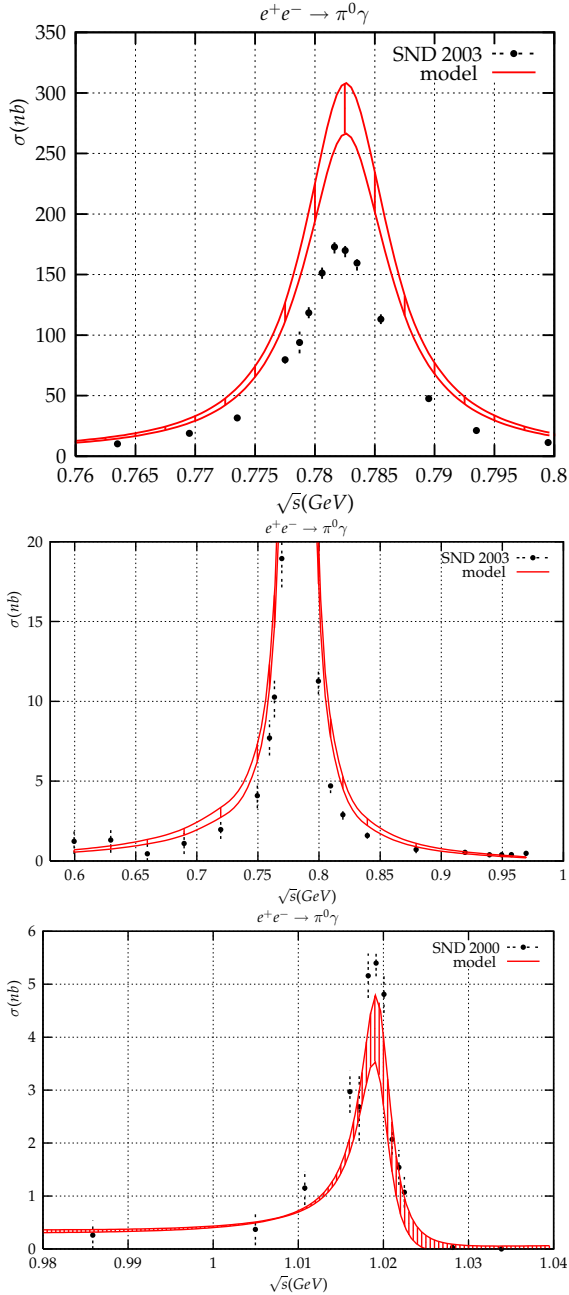


**Fig. 8.** Differential cross section of the process  $e^+e^- \rightarrow \pi^0\gamma$ . Data from Refs.[23] (SND 2003) and [24] (SND 2000) are shown together with  $1\sigma$  allowed bands for our model predictions.

known analytical results, where all photon angles are integrated, similarly to previously performed tests for other hadronic channels (see [7, 8, 9, 4]). The independence of the result from the soft photon separation parameter was also checked.

## 5 Summary and Conclusions

The Monte Carlo event generator PHOKHARA has been extended to the three-pion mode. The model adopted for

the hadronic form factor properly describes the currently available data for the cross section and the distributions. The ansatz is based on generalized vector dominance and is consistent with various other measurements like  $\Gamma(\pi^0 \rightarrow \gamma\gamma)$ , the slope parameter of the  $\pi^0 \rightarrow \gamma\gamma^*$  amplitude and radiative vector meson decays  $\rho \rightarrow \pi^0\gamma$ ,  $\phi \rightarrow \pi^0\gamma$ , but is in conflict with  $\omega \rightarrow \pi^0\gamma$ .

The current version of the computer program (PHOKHARA 5.0) is available at

<http://cern.ch/german.rodriego/phokhara>

## Acknowledgements

The authors thank J. Portolés for very helpful discussions and comments on the manuscript.

## References

1. Min-Shih Chen and P. M. Zerwas, Phys. Rev. D **11** (1975) 58.
2. S. Binner, J. H. Kühn and K. Melnikov, Phys. Lett. B **459** (1999) 279 [hep-ph/9902399].
3. H. Czyż, J. H. Kühn, E. Nowak and G. Rodrigo, Eur. Phys. J. C **35** (2004) 527 [hep-ph/0403062].
4. H. Czyż, A. Grzeźlińska, J. H. Kühn and G. Rodrigo, Eur. Phys. J. C **39** (2005) 411 [hep-ph/0404078].
5. G. Rodrigo, A. Gehrmann-De Ridder, M. Guillaume and J. H. Kühn, Eur. Phys. J. C **22** (2001) 81 [hep-ph/0106132].
6. J. H. Kühn and G. Rodrigo, Eur. Phys. J. C **25** (2002) 215 [hep-ph/0204283].
7. G. Rodrigo, H. Czyż, J.H. Kühn and M. Szopa, Eur. Phys. J. C **24** (2002) 71 [hep-ph/0112184].
8. H. Czyż, A. Grzeźlińska, J. H. Kühn and G. Rodrigo, Eur. Phys. J. C **27** (2003) 563 [hep-ph/0212225].
9. H. Czyż, A. Grzeźlińska, J. H. Kühn and G. Rodrigo, Eur. Phys. J. C **33** (2004) 333 [hep-ph/0308312].
10. M. Gell-Mann, D. Sharp and W. G. Wagner, Phys. Rev. Lett. **8** (1962) 261.
11. S. Eidelman *et al.* Phys. Lett. B **592** (2004) 1.
12. H. Czyż and J. H. Kühn, Eur. Phys. J. C **18** (2001) 497 [hep-ph/0008262].
13. R. Decker, P. Heiliger, H. H. Jonsson, M. Finkemeier, Z. Phys. C **70** (1996) 247 [hep-ph/9410260].
14. R. R. Akhmetshin *et al.* [CMD-2 Collaboration] Phys. Lett. B **578** (2004) 285 [hep-ex/0308008]; Phys. Lett. B **434** (1998) 426; Phys. Lett. B **364** (1995) 199.
15. M. N. Achasov *et al.* [SND Collaboration] Phys. Rev. D **68** (2003) 052006 [hep-ex/0305049]; Phys. Rev. D **66** (2002) 032001 [hep-ex/0201040].
16. S. I. Dolinsky *et al.* [CMD, ND, ARGUS Collaboration] Phys. Rept. **202** (1991) 99-170.
17. A. Cordier *et al.* [DM1 Collaboration] Nucl. Phys. B **172** (1980) 13.
18. A. Antonelli *et al.* [DM2 Collaboration] Z. Phys. C **56** (1992) 15.
19. B. Aubert *et al.* [BaBar Collaboration] Phys. Rev. D **70** (2004) 072004 [hep-ph/0408078].



20. A. Bramon, A. Grau, G. Pancheri, in “The second DAPHNE physics handbook.” p.477, SIS - Pubblicazioni dei LNF (1995), eds. L. Maiani, G. Pancheri, N. Paver.
21. M. Harada, K. Yamawaki Phys. Rept. **381** (2003) 1 [hep-ph/0302103].
22. P. D. Ruiz-Femenia, A. Pich and J. Portoles, JHEP **0307**, 003 (2003) [arXiv:hep-ph/0306157]; Nucl. Phys. Proc. Suppl. **133**, 215 (2004) [arXiv:hep-ph/0309345].
23. M. N. Achasov *et al.* Phys.Lett.B **559** (2003) 171 [hep-ex/0302004].
24. M. N. Achasov *et al.* Eur.Phys.J.C **12** (2000) 25.
25. The unpublished double precision version of RANLUX written by M. Lüscher (F. James - private communication):  
M. Lüscher Comput.Phys.Commun.79:100-110,1994 [hep-lat/9309020]; F. James, Comput.Phys.Commun. **79** (1994) 111.